Connection element for modeling of post-tensioned self-centering steel frames

Yasser Eljajeh[1], and Mihail Petkovski[2]

[1] BSc, MSc, Graduate research student. The University of Sheffield, Sheffield, UK

[2] MEng, MSc, PhD, Lecturer. The University of Sheffield, Sheffield, UK

ABSTRACT: Modeling of post-tensioned steel beam-column connections has been a subject of research since they were first introduced (Ricles et al. 2001) and several modeling techniques have been proposed to simulate the post-tensioned connection both locally and as a part of frame structures. This paper presents a connection element that can be used for modeling of post-tensioned steel frames. The model was built using the basic concepts of the connection behavior. This model can self-center upon unloading and switch between elastic and inelastic phases. In contrast with existing connection models which can be included in a frame analysis (Christopoulos et al. 2002), this model captures the gap opening event. First, the connection model was examined at the local level and its moment-rotation behavior showed the expected flag-shaped hysteresis. Then, the model was incorporated in a 2D frame model of a frame analysis program. Simulations of the incorporated element under a set of earthquake time histories exhibited a good self-centering behavior for the connection and the frame. In addition, the model provides the tension forces in each strand in the connection.

1   INTRODUCTION

Since post-tensioned connections were first introduced, a few modeling approaches have been proposed to analyze their behavior at both local and global levels. Post-tensioned connections can be modeled by using three modeling techniques (Kim and Christopoulos, 2009): (a) sectional analysis of post-tensioned steel connections, (b) a discrete springs model, and (c) a finite element model. Both the sectional analysis model and the finite element model aimed to study the connection components. The finite element modeling was used to study the stresses and the expected failure modes of post-tensioned steel beam-column connections (Esposto, 2008). Several finite element models created for the post-tensioned connections indicated that finite element modeling has high ability of simulating deformations and stress-state of all elements involved in the connection, high accuracy of response results, and high ability of simulating different types of failures that cannot be captured when using other techniques. Finite element modeling however, involved one main disadvantage. This approach is very expensive from computational point of view. Hence, it is suitable only for standalone connections, but not for incorporating the model into full frame analysis.

A computationally more efficient approach is to use a discrete springs model. This model gives a good representation of the behavior of the connection (Ricles et al. 2001), but is cumbersome, as it requires a large number of nodes and elements to be defined in the input. Attempts were made to provide a simple model by using only one rotational spring (Christopoulos et al. 2002

and Tsai et al. 2005), but this approach is not able to capture the gap opening event (Dobossy et al. 2006).

This paper presents an integrated connection element model (single-spring) that is simple to incorporate into frame model, and yet it can capture all the important events in the post-tensioned connection.

2 MOMENT-ROTATION RELATIONSHIP OF A POST-TENSIONED STEEL BEAM-COLUMN CONNECTION

The behavior of post-tensioned steel beam-column connections when subjected to dynamic loading is characterized by two main phases: elastic phase and inelastic phase. The connection behaves as elastic as long as the applied moment M_c of the connection is less than the moment causing the yielding of the energy dissipating bars (M_y) (Figure 1.a).

The stiffness of the connection in the elastic phase (k_0) is very high when $M_c < M_{st}$ due to the post-tensioning effect. Once the applied moment exceeds M_{st}, the stiffness drops to k_1, where $k_1 << k_0$. The stiffness k_1 is the sum of the stiffness of the post-tensioned strands (k_s) and the stiffness of the energy dissipating bars (k_b).

The connection behavior becomes inelastic when the yielding moment (M_y) is exceeded. The stiffness of the connection in this phase is dependent upon the loading/ unloading status of the connection. In order to specify the stiffness of the connection during the inelastic phase, the yield-status-time-increment technique is used (Cheng, 2001). In this technique the applied moment is compared to the yielding moment, that varies during the loading history. Stiffness of the connection in the next step depends on whether the connection is subjected to loading or unloading (Figure 1.b).
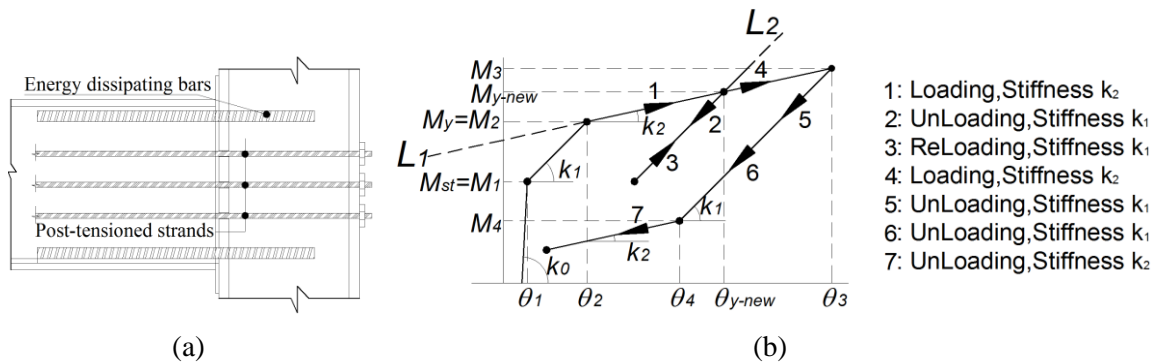

(a)	(b)

Figure 1. (a) Arrangement of the connection, and (b) moment-rotation relationship of the connection.

The most important feature of the connection's moment-rotation relationship is its ability to self-center after undergoing inelastic deformations. Elements with self-centering ability can switch between elastic and inelastic phases. The element may undergo inelastic deformations, and then self-center upon unloading and return to the elastic phase.

3 MODELING OF THE STANDALONE INTEGRATED POST-TENSIONED STEEL BEAM-COLUMN CONNECTION (IPTC)

3.1 Elastic phase of post-tensioned connection model

When the connection is working in the elastic phase, the rotation $\theta_l=0$ (infinite stiffness prior to gap opening $M_c <M_{st}$). Once the gap is opened, the stiffness drops to k_1 for $M_{st} <M_c<M_y$.

Loading-unloading follow the same path with no inelastic deformations. In the model, the infinite initial stiffness is replaced by a finite, very high value k_0 ($k_0 = C k_s$, $C \gg 1$). The higher is the initial stiffness (k_0), the closer θ_1 is to zero, and the more the model is prone to having numerical errors. Therefore, the value of k_0 should be carefully selected to avoid numerical instability while providing acceptable accuracy. The flowchart of the elastic phase is presented in Figure 2.
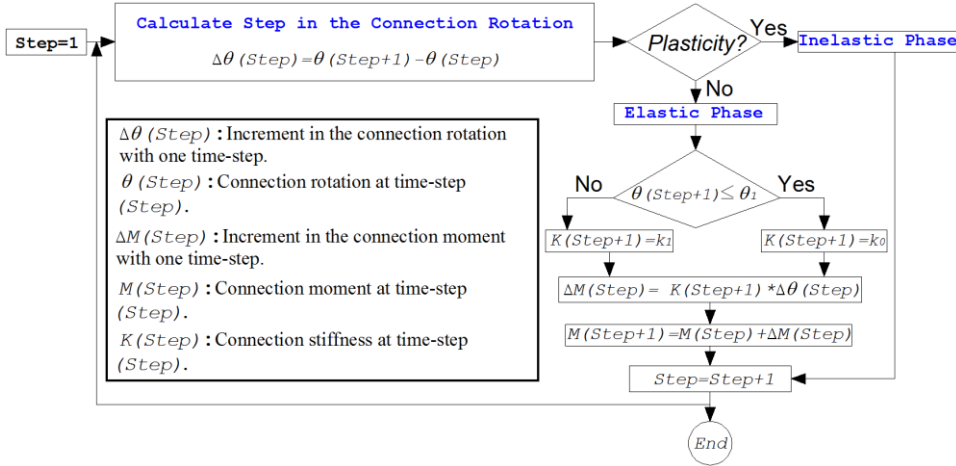

Figure 2. Flowchart of the elastic phase of the post-tensioned connection model.

3.2   *Inelastic Phase of Post-tensioned Connection Model*

The first time $\theta > \theta_2$, the connection enters the inelastic phase in which $k=k_2$, and which extends to $\theta_{y\text{-}new}$ and $M_{y\text{-}new}$. If the connection is unloaded, the stiffness changes and new points of the hysteresis are calculated ((θ_3,M_3), (θ_4,M_4), and (θ_5,M_5)). If $M_c > M_4$ the unloading-reloading stiffness returns again to k_1, if $M_c < M_4$, the unloading stiffness is reduced to k_2. If the connection starts re-loading, $\theta_{y\text{-}new}$ and $M_{y\text{-}new}$ are calculated and the reloading stiffness is k_1.
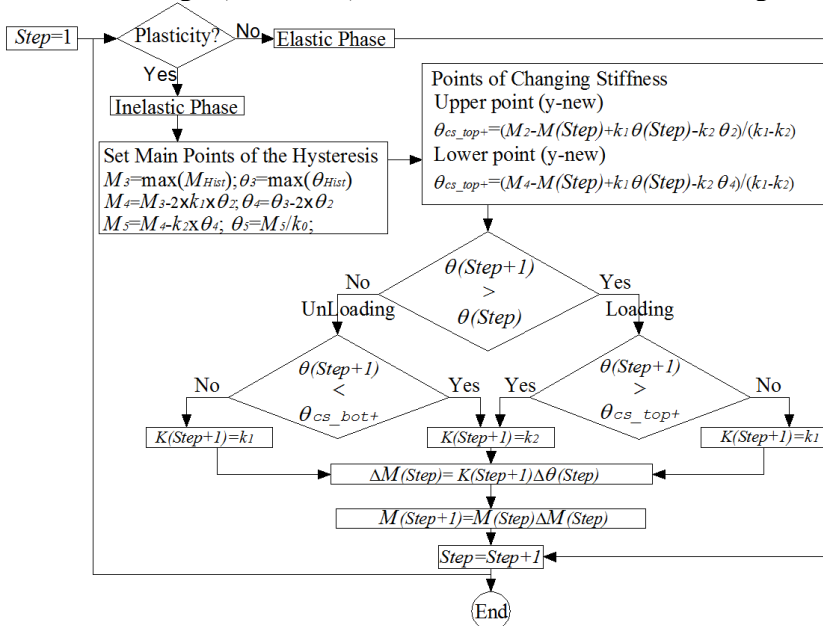

Figure 3. Flowchart of the inelastic phase of the post-tensioned connection model.

3.3   *Modeling of Self-Centering Characteristics of the Post-tensioned connection*

The first step is determining the rotation angle at which the connection self-centers. In reality, the self-centering angle is zero, but since the initial stiffness k_0 is not infinite, the self-centering rotation angle takes a non-zero value $|\theta_{sc}| < |\theta_l|$. At each time step, the self-centering angle can be positive (θ_{Sc+}) or negative (θ_{Sc-}).

Moments and rotations between two self-centering events (between gap-opening and gap-closing) are saved in vectors M_{Hist} and θ_{Hist}, which are then used to calculate the new points of the hysteresis ((θ_3, M_3), (θ_4, M_4), and (θ_5, M_5)) as shown in the diagram in Figures 1 and 3.

4   VERIFICATION OF THE IPTC MODEL USING A DISCRETE SPRINGS MODEL

To verify the new integrated model of post-tensioned connection, its performance was compared with a discrete springs model using DRAIN 2DX (Prakash et al.1993). The simulations were carried out for a post-tensioned connection between beam UB 610x305x179 and column UB 686x254x170, energy dissipating bars H20, f_y =240 MPa, strands with area A_s = 560 mm^2 and post-tensioning force F_{pt}= 300 kN. The moment-rotation relationships from the integrated post-tensioned connection model (IPTC) and the discrete springs model using DRAIN 2DX, under the same loading, are shown in Figure 4.
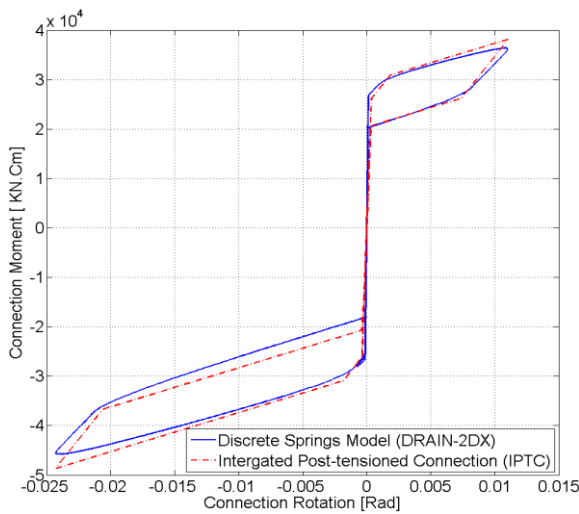

Figure 4. Verification of the post-tensioned connection model using the discrete springs model.

Figure 4 shows a good agreement between the idealised integrated hysteretic model (IPTC) and the discrete springs model. The gap-opening moments, the maximum rotations and the moments at which the energy dissipating bars start yielding are very similar. This comparison suggests that the idealised model gives an acceptable level of accuracy and can be used in simulations.

5   INCORPORATING THE STANDALONE IPTC MODEL INTO A 2D STEEL FRAME

In order to incorporate the post-tensioned connection model, a structural analysis program for two-dimensional frames (FASAC-2D) has been developed.

5.1   *Geometry and input data of the incorporated post-tensioned connection element (IPTC)*

The IPTC element in FASAC-2D is a zero-length element connecting one node of the column to the adjacent node of the beam.. Input data of the connection element are shown in Table 1.

Table 1. Input data for the IPTC element in FASAC-2D.

Parameter	Variable	Description
Energy dissipation	EDTY	Type of the energy dissipater: 1. yielding, and 2. friction.
Energy dissipation properties	D_b	Depth of the beam.
	E_b	Modulus of elasticity of energy dissipater (only for EDTY=1)
	f_{yb}	Yield stress of the energy dissipater (only for EDTY=1)
	F_{ved}	Slip force of friction-based energy dissipater (only for EDTY=2)
	L_b	Length of the energy dissipating bars (only for EDTY=1)
	dia	Diameter of the energy dissipating bars (only for EDTY=1)
	E_2/E	Ratio of post-yielding to pre-yielding stiffness of the energy dissipating bars (only for EDTY=1).
	C	Initial Stiffness factor.
	FricLoc	Location of the friction-based damper: (1) flanges, and (2) web.
Post-tensioned strands properties	N_{os}	Number of the strands in the post-tensioned connection.
	E_s	Modulus of elasticity of the strands
	f_{ys}	Yield stress of the strands.
	A_s	Area of the strand's cross section.
	L_s	Length of the strands adjacent to the connection*.
	F_{pti}	Initial post-tensioning force applied to the connection.

$*L_s$ depends on whether the connection is at external or internal column.

5.2 Operation of the IPTC element in the frame for Dynamic Analysis

When the gap in the connection is closed, parameter *YieldCode* is zero, the rotational stiffness is k_0, and the stiffness matrix of the connection element $[k_e]$ is presented in Equation (1):

$$[k_e] = \begin{bmatrix} k_0 & 0 & 0 & -k_0 & 0 & 0 \\ 0 & k_0 & 0 & 0 & -k_0 & 0 \\ 0 & 0 & k_0 & 0 & 0 & -k_0 \\ -k_0 & 0 & 0 & k_0 & 0 & 0 \\ 0 & -k_0 & 0 & 0 & k_0 & 0 \\ 0 & 0 & -k_0 & 0 & 0 & k_0 \end{bmatrix} \tag{1}$$

After solving the dynamic equations (using Newmark integration method; Chopra, 1995), the element deformations in local coordinates are calculated as:

$$\theta = \theta_{beam} - \theta_{col} \tag{2}$$

Here θ is rotation of the post-tensioned connection, θ_{beam} is rotation of the connection at the beam end and θ_{col} is rotation of the connection at the column end. The rotation of the connection θ is then used to calculate the moment of the connection from the IPTC model. The axial and shear forces in the connection are calculated directly from the local stiffness matrix of the connection element.

Once the moment in the connection is calculated in the first iteration, it is used to determine the value of *YieldCode* which is then employed to determine the new stiffness matrix of the connection element for the next iteration (Table 2).

Table 2. Connection stiffness matrix for different *YieldCode* values.

$$[k_e] = \begin{bmatrix} k_0 & 0 & 0 & -k_0 & 0 & 0 \\ 0 & k_0 & 0 & 0 & -k_0 & 0 \\ 0 & 0 & k_r & 0 & 0 & -k_r \\ -k_0 & 0 & 0 & k_0 & 0 & 0 \\ 0 & -k_0 & 0 & 0 & k_0 & 0 \\ 0 & 0 & -k_r & 0 & 0 & k_r \end{bmatrix}$$

YieldCode=0 ... $k_r = k_0$
YieldCode=1 ... $k_r = k_1$
YieldCode=2 ... $k_r = k_2$

k_0, k_1, and k_2 are shown in Figure 1.

The new stiffness matrix of the connection is used to assemble the modified global stiffness matrix of the frame. This process is repeated until the point at which the stiffness matrices of all elements are the same in two consecutive iterations, when the analysis moves to the next time step. The sign convention and calculation of the internal forces of the IPTC element are shown in Figure 5.
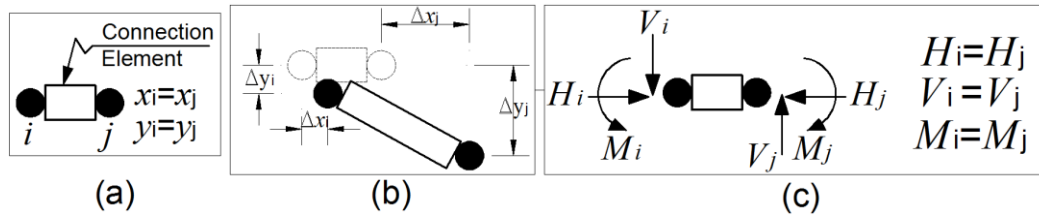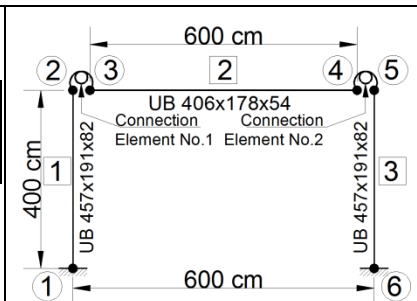

Figure 5. The IPTC element in FASAC-2D (a) undeformed shape, (b) deformed shape and (c) internal forces.

6   DYNAMIC ANALYSIS OF A STEEL FRAME EQUIPPED WITH THE IPTC MODEL

A portal frame was upgraded with the IPTC element (Table 3), and analysed for a set of four records: El-Centro (elcn40ns -1940), Mexico City (mexico_sct1_021 -1985), Loma-Prieta (LOMAP/CAP000-1989), and Northridge (NORTHR/HOS090 -1994).

Table 3. Properties and arrangement of the IPTC element in the frame under consideration .

Energy Dissipation Type: *EDTY* = 1; Energy Dissipation Properties (kN,cm)								
D_b	E_b	f_{yb}	F_{yed}	L_b	dia	$E2/E$	C	*Fric Loc*
40.3	2.1e3	24	150	100	2.00	0.2	80	1
Post-tensioned Strands Properties (kN,cm)								
N_{oS}	E_s	f_{ys}	A_s	L_s	F_{pti}			
40.3	2.1e3	24	150	100	2.00			

6.1   Moment-Rotation Relationship of the Post-tensioned Steel Beam-Column Connections

The moment-rotation response of connection element No.1 is presented in Figure 6, in which, three response stages have been mobilised: (k_0) before gap opening, (k_1) elastic, after gap opening and (k_2) inelastic phase. In all cases the connection self-centers at the end of the simulation (as expected) and shows no residual rotations.
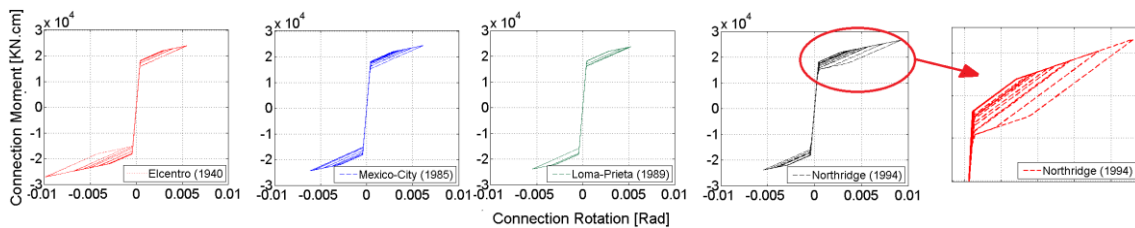

Figure 6. Moment-rotation relationship for the incorporated connection element.

6.2   Global Response of Frame

The comparison of horizontal displacements of the conventional moment resistant frame and the frame equipped with the IPTC connection under Loma-Prieta earthquake (Figure 7) shows that the IPTC reduces the residual displacements of the frame from 12.5 mm to 3.7 mm (70.4%).
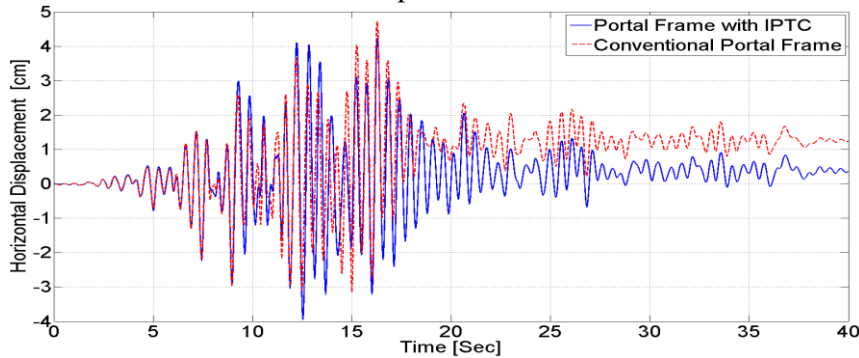

Figure 7. Horizontal displacements of conventional frame and frame with the IPTC element.

6.3   Tension Forces in the Strands of the Connection Element

One of the advantages of the IPTC model is that it enables direct calculation of the tension forces in the strands, based on their elongation due to rotation of the connection. In Figure 8 are shown deformations of the strands for positive and negative rotations.
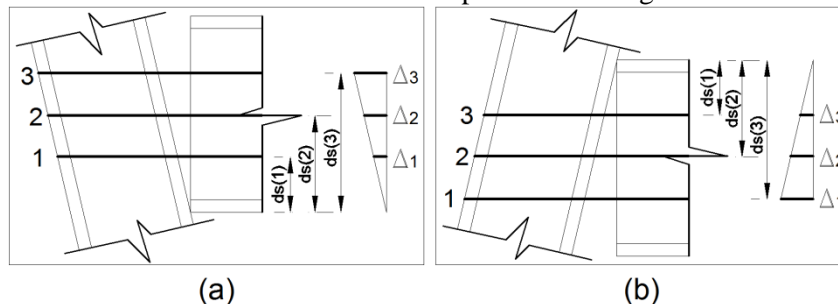

Figure 8. Strands deformations due to connection's rotation. (a) positive rotation and (b) negative rotation.

Conclusions

In this paper is presented an integrated post-tensioned steel beam-column connection element (IPTC) for modeling of post-tensioned steel frames. The purpose of this model is to provide the moment-rotation relationship of the post-tensioned connection by using a single element that is computationally efficient, can be easily incorporated in a frame model, represents all phases of the response and provides data for design of the individual components of the connection . The most important feature of this model is its ability to self-center upon unloading. The IPTC model captures all the important events in the post-tensioned connections. When incorporated in a 2D post-tensioned steel frame, the IPTC model shows the expected flag-shaped moment-rotation relationship. The simulations of four earthquake time histories show self-centering of the frame and reduced residual deformations. Also, the IPTC model computes the post-tensioning forces in the strands which can be used for designing the connection.

References

Cheng F. 2001. *Matrix Analysis of Structural Dynamics, Applications and Earthquake Engineering*. Chapter 9. New York, MARCEL DEKKER, INC.

Chopra A K. 1995. *DYNAMICS OF STRUCTURES: Theory and Applications to Earthquake Engineering*. Chapter 15. New Jersey, PRENTICE HALL.

Christopoulos C, Filiatrualt A, Uang C, and Folz B. 2002. Posttensioned Energy Dissipating Connections for Moment-Resisting Steel Frames. *Journal of Structural Engg*. 128: 1111-1120.

Dobossy, M, Garlock, M, and VanMarcke, M. 2006. Comparison of Two Self-Centering Steel Moment Frame Modeling Techniques: Explicit Gap Models and Non-Linear Rotational Spring Models". *4th Int. Conference on Earthquake Engg*. Taipei, Taiwan. Paper No.101.

Esposto M. 2008. *PTED BEAM-TO-COLUMN CONNECTIONS FOR STEEL MOMENT RESISTING FRAMES: STRUCTURAL IDENTIFICATION BASED ON NUMERICAL ANALYSES*. PhD Thesis, Università degli Studi di Napoli Federico II, Naples, Italy.

Kim H and Christopoulos C. 2009. Numerical models and ductile ultimate deformation response of post-tensioned self-centering moment connections. *Earthquake Engg. and Structural Dynamics*. 38:1–21.

The Regents of the University of California. 2005. Pacific Earthquake Engineering Research Center: NGA Database. Available at: http://peer.berkeley.edu/nga/search.html

Prakash V, Powel, G,H, and Campbell, S. 1993. *DRAIN-2DX Base Program Description and User Guide.*

Ricles J, Sause R, Garlock M, and Zhao C. 2001. Posttensioned Seismic-Resistant Connections for Steel Frames. *Journal of Structural Engg*. 127(2):113-121.

Tsai K, Chou C C, and, Jhuang S J. 2005. Seismic response of structural systems using self-centering connections. *US-Taiwan Workshop on Self-Centering Structural Systems*.